Ali Hasan Mousa, MOHD AZLISHAH BIN OTHMAN, Mohamed Zoinol Abidin, Ayman Mohammed Ibrahim

Universiti Teknikal Malaysia Melaka (UTeM), Malaysia, Malaysia

doi:10.15199/48.2021.06.03

Fractal H-Vicsek MIMO Antenna for 5G Communications

Abstract. *A Fractal H-vicsek MIMO antenna was designed in the band of 3.3 – 3.7 GHz for 5G applications is demonstrated in this paper. The proposed antenna is printed on a FR4 substrate material with relative permittivity of 4.3 and height of 0.8 mm, and dimension of the antenna was 12.5 × 37 × 0.8 mm^3. This paper presents the development of a compact MIMO antenna using a new structure integrated with the H-shaped using neutralization line and defected ground structure techniques for mutual coupling reduction and antenna isolation improvement. The simulated results proved that the proposed method gives an excellent isolation performance. A good impedance matching return loss of large than 10 dB, high isolation of large than 16 dB at the operating frequency, and low ECC that was 0.009 was simulated across the coveted operating bandwidth.*

Streszczenie. *W artykule przedstawiono antenę Fractal H-vicsek MIMO w paśmie 3,3 - 3,7 GHz do zastosowań 5G. Proponowana antena jest drukowana na materiale podłoża FR4 o przenikalności względnej 4,3 i wysokości 0,8 mm, a wymiary anteny wynosiły 12,5 × 37 × 0,8 mm3. W artykule przedstawiono opracowanie zwartej anteny MIMO wykorzystującej nową konstrukcję zintegrowaną z kształtem litery H za pomocą linii neutralizacji oraz technik uszkodzonej struktury gruntu w celu redukcji wzajemnych sprzężeń i poprawy izolacji anteny. Symulowane wyniki dowiodły, że proponowana metoda zapewnia doskonałą izolację. W pożądanym paśmie roboczym zasymulowano dobre dopasowanie impedancji tłumienia odbicia powyżej 10 dB, wysoką izolację powyżej 16 dB przy częstotliwości roboczej i niskie ECC, które wynosiło 0,009. (**Fractalna H-Vicsek MIMO Antena dla komunikacji 5G**)*

Keywords: 5G band, Envelope correlation coefficient (ECC), Fractal antenna, Isolation, 5G, MIMO antenna.
Słowa kluczowe: antena szerokoasmowa, pasmo 5G, antena fraktalna

Introduction

Over the past three decades, improvements in cellular communications standards have dramatically altered the construction of antennas. Two main parts are included in this development. First, it is the interest of users, which consists mainly of ergonomic and aesthetic considerations, and secondly, the introduction of different spectra in line with evolving regulatory standards. Antenna design is one of the many difficult requirements for mobile system designers[1]. The rapid growth of mobile wireless systems requires multi-band, broadband, or even broadband antennas to cover the interoperability of mobile services and reduce system complexity. Additional demands for portable antennas include small size, ease of integration into the portable chassis, and coexistence with and support for MIMO systems. MIMO is one of the key elements that support 5G technology in achieving better bandwidth compared to 4G and LTE systems[2]. This technology provides additional system capacity while increasing the number of antenna elements, without the need for additional frequency or power spectrum. A high-performance MIMO system requires high isolation for each element and a low envelope correlation coefficient between them. However, this needs to be spaced between items, which is difficult to find in mobile devices as it is ideally designed to be compact antenna design[1]-[3].

At the same time, antennas are needed to be placed closer to each other as there is a constraint of space as well. As the antennas are placed closer to each other, the near field effect dominates in the form of surface and space waves, giving rise to strong mutual coupling among the antennas. This causes a decrement in antenna efficiency, bandwidth, and gain. The existence of mutual coupling degrades the maximum achievable performance of the communication system. Besides, the design of MIMO antennas over a limited space requires various approaches for the reduction of mutual coupling, otherwise the gain, efficiency, diversity gain and radiation patterns would be severely affected [3]. Thus, the mutual coupling reduction techniques should be applied with greater care, and other parameters must be considered. One of the possible solution to the problem of mutual coupling is the use of isolation techniques. The isolation decreases the mutual coupling among antenna elements and improve the gain and efficiency of the system [2]–[4]. As such, this paper attempted to solve the above-mentioned issues with a high isolation printed on two-element arrays operating in the centre frequency of 3.6 GHz in the band of 3.3-3.7 GHz

Antenna Design and Analysis

Fractals theories perform a role in describing the features of complex systems in nature since many things in the real world can be modelled by fractals. So, a fractal is a model that returns itself at smaller then smaller scales and to result in an irregular shape. The geometrical shape of the rectangular patch with a crossed fractal is shown in Fig.1. The basic design parameters for the rectangular shape are the dimensional width 12.5 mm and the length 37 mm. The design is achieved using the FR-4 substrate with thickness ht = 0.0.035 mm and relative permittivity (εr = 4.4). The width of the microstrip patch antenna is calculated using equation (1)[5]:

$$W = \frac{c}{f_r\sqrt{\frac{\epsilon_r+1}{2}}} \tag{1}$$

The effective constant Ɛreff is calculated by using equation (2)[5]:

$$\epsilon_{reff} = \frac{\epsilon_r+1}{2} + \frac{\epsilon_r-1}{2}\left(1+12\,\frac{h}{w}\right)^{\frac{-1}{2}} \tag{2}$$

where effective length Leff can be calculated by equation (3) [5]:

$$L_{eff} = \frac{c}{2f_r\sqrt{\epsilon_{reff}}} \tag{3}$$

The fringing length (ΔL) is calculated by equation (4):

$$\Delta L = 0.412\frac{(\epsilon_{reff}+0.3)(\frac{w}{h}+0.264)}{(\epsilon_{reff}-0.258)(\frac{w}{h}+0.8)} \tag{4}$$

The length of the patch (L) for proposed microstrip antenna is composed of a rectangular patch, FR-4 substrate, the actual length of a patch is given by equation (5):

$$L = L_{eff} + 2\,\Delta L \tag{5}$$

Calculation of the ground plane dimensions is given by equations (6) and (7):

(6) Lg = 6 × ht + L

(7) Wg = 6 × ht + L

In [5], the following empirical formula given in eaquation (8) was utilized to calculate the resonant frequency for rectangular patch:

(8) $$f_r = \frac{c}{2L\sqrt{\epsilon_{eff}}}$$

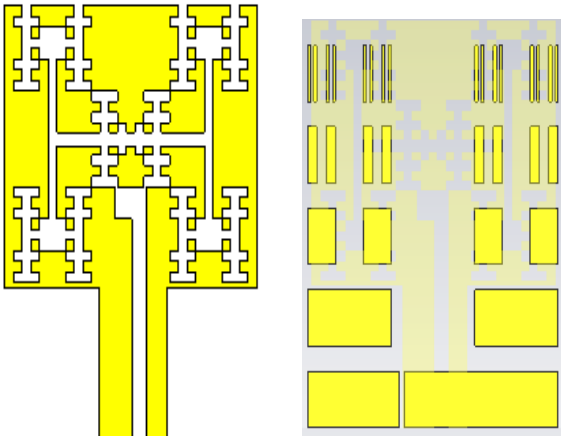

Fig.1: *A Fractal H-Vicsek single antenna*

The single of the proposed antenna is a rectangular antenna which was designed through a procedure consisting of five stages. In the first and second stages, a rectangular-shaped antenna (antenna 1 and antenna 2) were designed with dimensions of 12.5 × 37 mm^2 and 12.5 × 36.2 mm^2 respectively, as shown in Fig. 2(a) and (b). The operating frequency of the patch plane was calculated through Equation (8) [6].

In the third stage was designed (antenna 3) a vicsik-shaped antenna. This geometric of fractal shape starts out as a simple square-shaped and iteration order is zero (0th) as shown in Fig. 3(a). In iteration 1st, divided the square into four small equal squares and move it to the four corners as shown Fig. 3(b). In iteration 2nd, divided five squares into twenty small equal squares and move it to the four corners as shown in Fig. 3(c). In iteration this geometric of fractal shape starts out as a simple square-shaped and iteration order is zero (0th) as shown in Fig. 3(a). In iteration 1st, divided the square into four small equal squares and move it to the four corners as shown Fig. 3(b). In iteration 2nd, divided five squares into twenty small equal squares and move it to the four corners as shown in Fig. 3(c). In iteration 3rd, divided twenty-five squares into one hundred small equal squares and move it to the four corners as shown in Fig. 3(d). If the iterative process is performed, an unlimited number of times is obtained to an ideal fractal geometry called Vicsek-shaped. The shape of Vicsek has a limited area and an unlimited perimeter. To design a Vicsek fractal, the linear dimensions of the fractal are determined so that a fractal perimeter is determined by the boundary of the square fractal patch. The length of L1 is the x-axis side and y-axis side of the square, where L1=X=Y=10.8 mm. In Fig.3, can be analytic of the iterations by calculating the number of squares on patch plane. The number of slots squares in the Iteration 0th is 1 square. The total number of slots squares in the iteration 1st is 5 squares. While the total number of squares in the iteration 2nd is 5 × 5 = 25 square. Also, the total number of slots squares in the iteration 3rd is 5 × 5 × 5= 125 square, can be used the following equation to calculate the number of squares:

(9) $$Number\ of\ squares = 5^i$$

where, i=0, 1, 2. The next step is to calculate the perimeter of the iterations. In iteration 0th, the Primarily dimension of the original square starts with L1= 10.8 mm and thus the value of perimeter is 4 × L1= 10.8 × 4 which equals 43.2 mm.

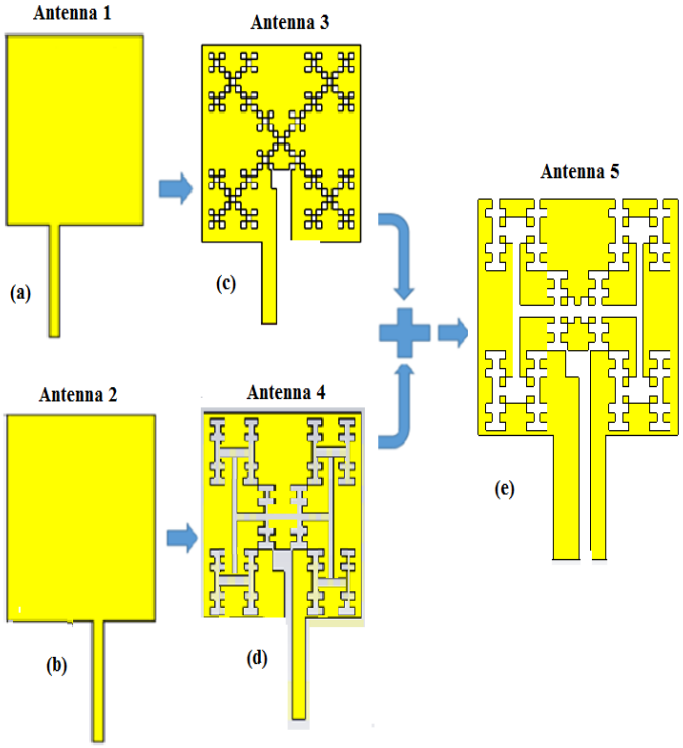

Fig.2: patch rectangular *H-Vicsek antenna*

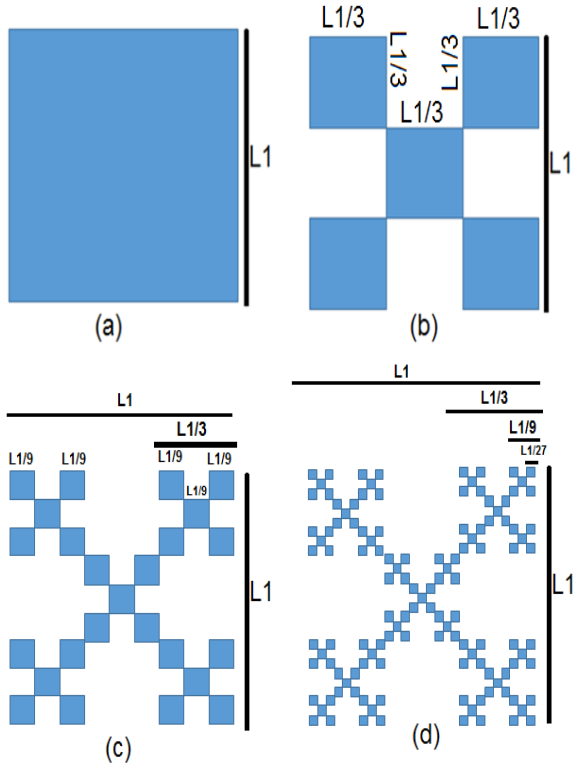

Fig.3: Configuration process for slot viscek-fractal. Rectangular 0th iteration, (b) Rectangular 1st iteration, (c) Rectangular 2nd iteration, and (d) Rectangular 3rd iteration.

Table 1 displays a relation between the perimeters of slots squares and the number of slots squares. The perimeter of the iteration 1st is L1/3 × 4 × 5 = 72. Also, the perimeter of the iteration 2nd is L1/9 × 4 × 25 = 120 mm. So, the perimeter of the iteration 3rd is L1/27 × 4 × 125 = 200 mm. can be used the following equation to calculate the perimeter of the iterations:

(10) Perimeter of iterations = small square of iteration × number of sides×number of squares

Perimeter of iterations

(11) $= \frac{L1}{3^i} \times 4 \times 5^i \quad where, i = 0, 1, 2$

Table 1: Relation between the perimeters of squares and the number of squares

Ite.	Length of square's side	Number of squares	Perimeter of squares
0	10.8	50 =1	10.8 × 4 × 1 = 43.2
1	5/3 = 3.6	51 =5	3.6 × 4 × 5 = 72
2	5/(3×3)=1.2	52 = 25	1.2 × 4 × 25 = 120
3	5/(3×3×3)=0.4	53 =125	0.4 × 4 × 125 = 200

In the fourth stage was designed (antenna 4) a H-shaped antenna. This geometric of fractal H-shaped starts out as a simple Line-shaped and iteration order is zero (0th) as shown in Fig. 4(a). In iteration 1st, created the three slots lines to form H-slot, as shown in Fig. 4 (b).In iteration 2nd, created the four slot lines and move it to the four corners as shown in Fig. 4(c). In iteration 3rd, added four forms of slots H-shaped and move it to the four corners as shown in Fig. 4(d). In iteration 2nd, created the sixteen slot lines and move it to the four corners as shown in Fig. 4(e). If the iterative process is performed, an unlimited number of times is obtained to an ideal fractal geometry called H-shaped. The shape of H-shaped has a limited area and an unlimited perimeter. To design an H-fractal, the linear dimensions of the fractal are determined so that a fractal perimeter is determined by the boundary of the rectangular fractal patch.

Fig. 2 shows the design method of (antenna 4) the H shaped fractal antenna, starting an H-shaped fractal antenna with length M5 and width M6. In Stage 1, the length of the horizontal strip (M1) is δ times L1, where δ is the scale factor with the value between 0 and 1. Hence, the M1 is smaller than M2 and M3 is smaller than M. However, the four vertical stripes are added to the two ends of the horizontal strip to form H character. The width of the four vertical strips is 0.4 mm, while is the width of M1 equal 2 mm. The same procedure is applied to all stages, as shown in Fig. 4. Lastly, the H–shaped fractal antenna is achieved at Stage 5, as shown in Fig. 4(e). The length of verticals and horizontals lines in each stage can be determined by Equation [7]:

(12) M (i+1) = δ (M (i). M (I =1, 2, …, 5)

The geometry of the H-shaped fractal antenna must be determined to avoid overlapping between slots-lines during creating the proposed fractal antenna. The scale factor δ can control the size of the antenna, is one of the key parameters affecting the impedances and resonances of the proposed fractal antenna. Equations (13) and (14) used for calculating the scale factor δ to avoid the overlapping [7]:

(13) $1 - \left[\sum_{s=3}^{N} \delta^{s-1}\right] > \frac{P_6}{M_4}$

(14) $1 - \left[\sum_{S=4}^{N} \delta^{S-2}\right] > \frac{2P_6}{M_4}$

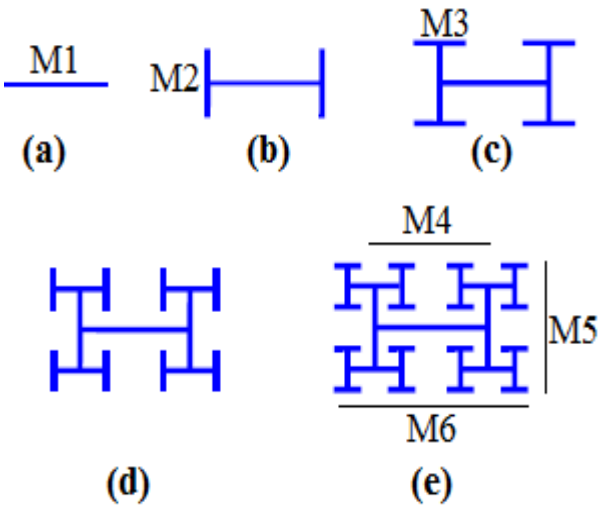

Fig.4 Configuration process for slot H-fractal. Rectangular 0th iteration, (b) Rectangular 1st iteration, (c) Rectangular 2nd iteration, (d) Rectangular 3rd iteration, and (e) Rectangular 4rd iteration

In the fifth stage was designed (antenna 5) an H-shaped antenna, combining between antenna 3 and antenna 4 to form antenna 5, as shown in Fig. 2(e).

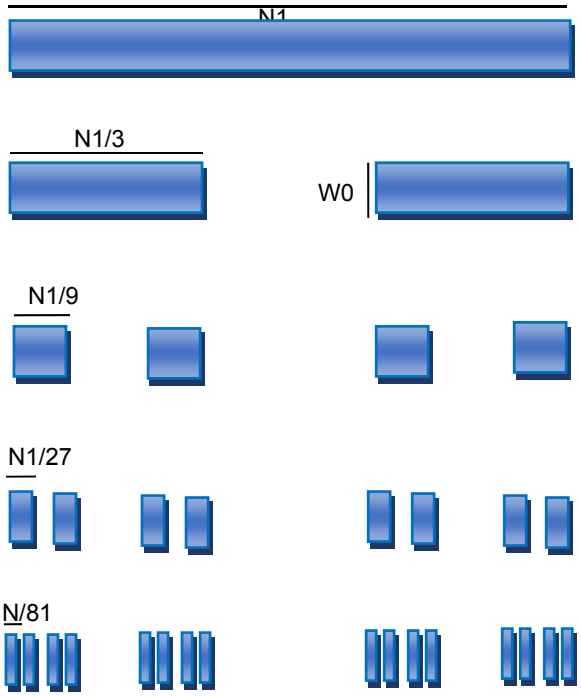

Fig.5 Configuration process for cantor set fractal of ground plane.

The geometry of the ground antenna depends on the technique of the Cantor set. A technique cantor set is a self-similar object which is formed by an iterative method beginning with of width and length. The initiator in the new proposed fractal antenna is a rectangular patch, as shown in Fig. 5(b). There are five stages to designing a ground plane with a cantor set technique. The first stage, design rectangular (N1) of dimensions length 12.5 mm and width 2.25 mm. The Second stage, divide the N1=12 mm into

three non-overlapping segments to formed three pieces of rectangular (N1/3) with the middle rectangular removed. Finally, This method is continued by repetitive application of the generator to each remaining layer[8].

Table 2 shows the dimensions of the designed fractal antenna. Which includes two-elements orthogonal of the MIMO antenna held a symmetrical monopoles antenna. This proposed MIMO antenna includes two separate ports with a distance of 2.8mm monopoles printed on a 12.5 × 37 mm FR-4 substrate, as exhibited in Fig. 6. To obtain high isolation, using defected ground structure (DGS) to the inserted two slots and three lines on the ground plane and neutralization line (NL) was inserted between the two separated antennae of the patch plane, as shown in Fig. 6. This complemented the Horizontal line of the ground plane, with a width of G2 = 0.4 mm and length of G1=12.5mm. With the vertical line slot of a width of G3 = 0.3 mm and length of W0 =2.25 mm.

Table 2: Parameters and dimensions of fractal Vicsek MIMO antenna (mm).

Parameter	Value	Parameter	Value	Parameter	Value
L	37	P3	8,25	G2	0.4
W	12.5	P4	5.65	G3	0.3
W0	2.25	P5	1.48	G4	7.34
M6	10.8	P6	0.7	G5	4.36
Fe	5.65	P7	0.9	L1	10.8
P1	9.45	P8	11.7	M1	2
P2	10.6	G1	12.5	M2	3.6
M3	1.2	M4	6.97	M5	10

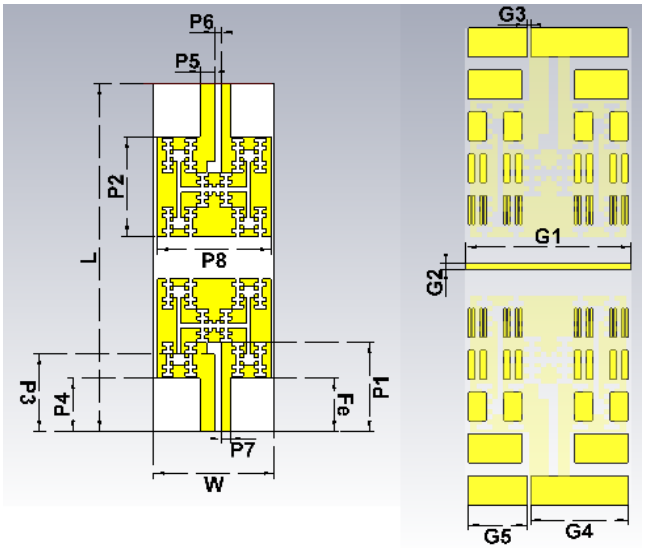

Fig. 6: Proposed design geometry of *Fractal H-vicsek MIMO antenna*

Performances MIMO antenna

The simulated reflection coefficients ($S11$) are shown in Fig. 7(a) and the fractal antenna isolations are shown in Fig. 7(b) for design. The fractal antenna has shown good response within the chosen frequency band. The simulated impedance bandwidth shows good coverage around the resonant frequency of 3.55 GHz. Also, a significant shift in $S11$ is given at a distance of 3 mm due to high coupling between the dual-element. The identical scenario is observed for antenna isolation, where at 3 mm, the isolation is becoming worse. In this paper, the main focus is to increase isolation between dual-element MIMO at the wanted band. From these results, the optimum fractal MIMO antenna in this work has been selected at 4.65 mm distance between dual-element due to its overall performance for 5G MIMO application.

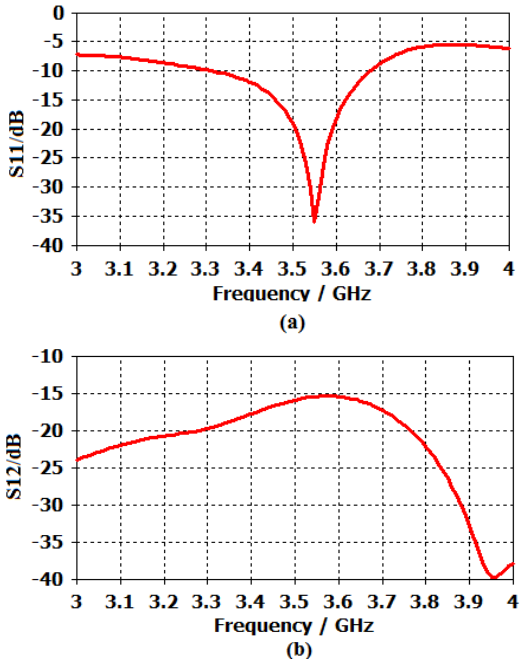

Fig. 7: S-Parameters of the H-vicsek MIMO antenna

In order to obtain high isolation, NL was inserted between the two separated antenna elements and DGS slot were inserted on the ground plane. The NL used a horizontal line and the slot line on the ground plane. In addition, the parametric study showed that the frequency response and bandwidth of the MIMO antenna are greatly influenced by slot width on t.e ground plane. An increase or decrease in the width of this slot was found to have induced a change in the centre resonant frequency of the design bandwidth, as shown in Fig. 8. As can be observed from Fig. 8, the isolation technique significantly increased the isolation between the antenna elements, by a significant reduction in S12 curve. Two Isolation techniques (NL and DGS) were used in the proposed antenna. The hybrid technique reduced the coupling in the ground plane and thereby, increased isolation between the antenna elements. Adding to that, the antennas were placed vertically, 4.65 mm apart, which further enhances the isolation between the antenna elements.

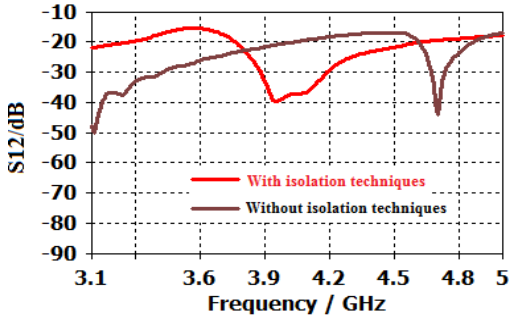

Fig. 8: Isolation (a) without and (b) with isolation techniques

A maximum envelope correlation coefficients (ECC) obtained was 0.009 for the three bands (3.3 - 3.7) GHz for 5G applications, as shown in Fig. 9. An addition that, A good level of efficiency 40-48% was obtained from the respective operating band, and the efficiency of the proposed MIMO antenna was above 40% in the operating band.

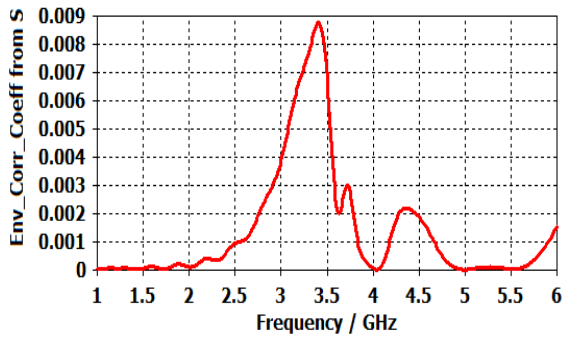

Fig. 9: Simulated ECC of the H-vicsek MIMO Antenna of Band (3.3 -3.7) GHz

Diversity gain (DG) is another important factor that must be taken into account while evaluating the performance of MIMO antenna system. It provides information about the reliability of the MIMO system. The higher value of diversity gain signifies better isolation between antenna elements. It depends on the correlation coefficients between antenna signals is given by the following Equation [9]:

$$\text{DG} = 10\sqrt{1-|\text{ECC}|^2} \quad (15)$$

Figure 11 shows the diversity gain of the proposed design, observed that the suggested MIMO antenna provides high DG > 10.

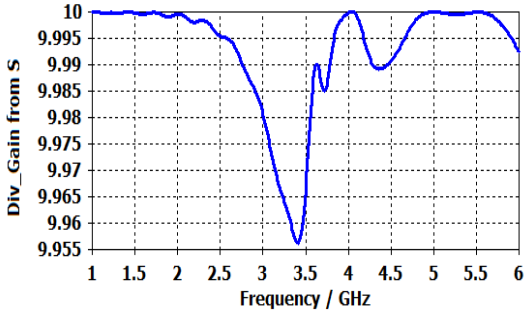

Fig. 10: DG of Disc MIMO Antenna

As shown in Fig. 6, the current in the input element was taken at a specific location where the impedance was minimum and the current was maximum, and then its phase was reversed by the hybrid isolation technique. This reverse current was then fed to the nearby antenna to reduce the amount of coupled current. The mutual coupling problem between the two antennas, was solved by NL method. From the surface current distribution in Fig. 11, it can be observed that the current is mainly concentrated in around of the slots, which generates inverse surface current and thus, reduces the coupling between the antenna elements.

Fig. 12 shows the simulated radiation pattern of the proposed MIMO antenna for a frequency of 3.5 GHz when Port 1 is excited.

Validation of the Proposed Antenna

Table 3 shows, the comparison of findings between this research works with other research work. The proposed antenna is compared with several selected types of research. The comparison was based on important characteristics, such as several ports, isolation, efficiency, envelope correlation coefficient, material, bandwidth and size. This V-shaped MIMO antenna is the best for LTE and 5G communications propose for several reasons.

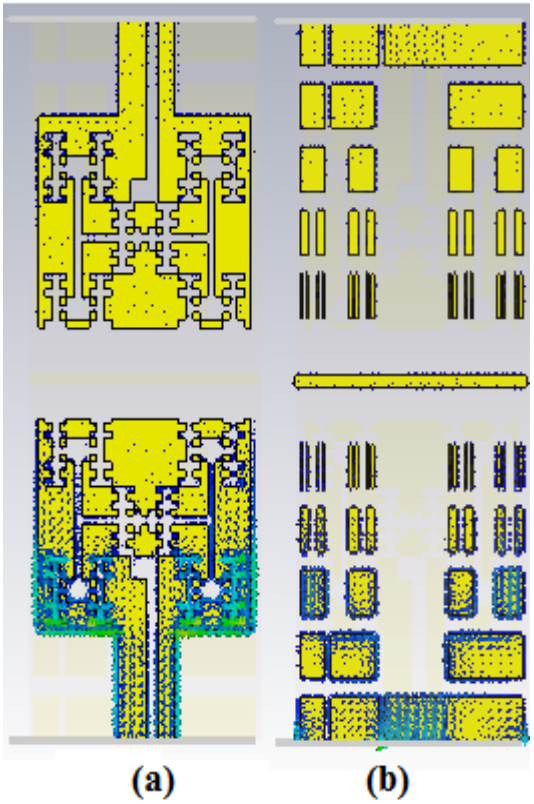

Fig. 11: Simulated current densities with port1 of the fractal H-vicsek mimo antenna (a) Top view (b) Back view

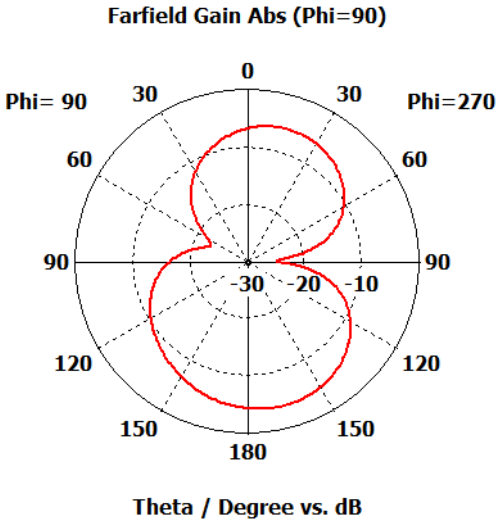

Fig. 12: Radiation Characteristics of proposed antenna at operating frequency 3.55 GHz.

Table 3: Comparisons between the proposed of MIMO antennas and previous related antennas

Ref.	BW (GHz),	Size (mm^2)	Isolation	ECC
[9]	(3.4–3.8)	60 × 25	15	< 0.02
[10]	(3.2–3.7)	60 × 40	23	<0.002
[11]	(3.6-3.8)	40.5×40.5	17	<0.035
[12]	(3.6-4.2)	31 × 31	10.5	< 0.0024
[13]	(3.6-3.99)	37 × 56	15	< 0.08
[14]	(3.4-3.8)	75×150	15	<0.05
[15]	(4.4-4.9)	21 × 24	18.5	< 0.15
[16]	(3.5–3.6)	40×100	15	<0.03
This work	(3.3-3.7)	12.5 × 37	16.5	<0.009

Conclusion

A mobile phone with a two-element antenna design was proposed for the use of 5G MIMO communications. This job involved the simulation of a novel fractal MIMO antenna for the band range of (3.3-3.7) GHz. The isolation was increased by way of the application of decoupling hybrid technique (neutralization lines and defected ground structure). Besides enhancing the isolation between the antenna elements, the ECC between the signals received by the MIMO antenna ports was sufficiently reduced to meet the specifications for 5G applications.

Acknowledgment

The authors would like to thank Centre for Telecommunication Research and Innovation (CeTRI), Research and Innovation Management (CRIM) and Universiti Teknikal Malaysia Melaka (UTeM) for their encouragement and help for supporting financially to complete this research work.

***Authors**:Ali Hasan Mousa, Email: alommousa75@gmail.com; Mohd Azlisha bin Othman, Email: azlishah@gmail.com; Mohamed Zoinol Abidin, Email: mohamadzoinol@utem.edu.my; Ayman Mohammed Ibrahim, Email: ayman971972@gmail.com.*

REFERENCES

[1] A. M. Ibrahim, I. M. Ibrahim, and N. A. Shairi, “Review Isolation Techniques of the MIMO Antenna for Sub-6,” Prozlad Elektrotechniczny, 2021, (01), pp.1-8.

[2] A. M. Ibrahim, I. M. Ibrahim, and N. A. Shairi, “Compact MIMO Antenna for LTE and 5G Communications,” Prozlad Elektrotechniczny, 2020, (10), pp.43-46.

[3] Panda, P.K. and Ghosh, D., “Isolation and gain enhancement of patch antennas using EMNZ superstrate. AEU-International Journal of Electronics and Communications, ” 2018, 86, pp.164-170.

[4] Malviya, L., Panigrahi, R.K. and Kartikeyan, M.V., “MIMO antennas with diversity and mutual coupling reduction techniques: a review. International Journal of Microwave and Wireless Technologies, ” 2017, 9(8), p.1763.

[5] Balanis,C. A., Antenna Theory Analysis And Design, 2016, 4th ed., Canada: Wiley.

[6] A. M. Ibrahim, I. M. Ibrahim, and N. A. Shairi, “Compact MIMO Antenna for LTE and 5G Applications. Int. J. Microw. Opt. Technol, ” 2020, 15(4), pp.360-368.

[7] Weng, W.C. and Hung, C.L., “An H-fractal antenna for multiband applications” IEEE Antennas and Wireless Propagation Letters, ” 2014, 13, pp.1705-1708.

[8] Manimegalai, B., Raju, S. and Abhaikumar, V., “A multifractal cantor antenna for multiband wireless applications,” IEEE Antennas and Wireless Propagation Letters, 2008, 8, pp.359-362.

[9] H. S. Singh, Shalini, and M. K. Meshram, “Printed Monopole Diversity Antenna for USB Dongle Applications,” *Wirel. Pers. Commun.*, 2016, 86, (2), pp. 771–787.

[10] K. V. Babu and B. Anuradha, “Design of Multi-Band Minkowski MIMO Antenna to Reduce the Mutual Coupling,” J. King Saud Univ. - Eng. Sci., 2018,6, (3), pp. 51-57.

[11] I. Suriya and R. Anbazhagan, “Inverted-A based UWB MIMO Antenna with Triple-band Notch and Improved Isolation for WBAN Applications,” Int. J. Electron. Commun. (AEÜ), 2019, 99,(5), pp. 25–33.

[12] A. M. Ibrahim, I. M. Ibrahim, and N. A. Shairi, “Compact Crecent Slot MIMO Antenna with Quad Bands and High Isolation for LTE and 5G communications,” Prozlad Elektrotechniczny, 2020, (12), pp.19-25.

[13] S. Chouhan, V. S. Kushwah, D. K. Panda, and S. Singhal, “Spider-shaped fractal MIMO antenna for WLAN/WiMAX/Wi-Fi/Bluetooth/C-band applications,” *AEU - Int. J. Electron. Commun.*, 2019,110, (3) p. 152871.

[14] N. O. Parchin et al., “Eight-Element Dual-Polarized MIMO Slot Antenna System for 5G Smartphone Applications,” IEEE Access,2019. 7,(53), pp. 15612–15622.

[15] A. M. Ibrahim, I. M. Ibrahim, and N. A. Shairi, “Compact MIMO Antenna for LTE and 5G Applications,” Prozlad Elektrotechniczny, 2020, (11), pp.84-89.

[16] C. F. Ding, X. Y. Zhang, S. Member, C. D. Xue, C. Sim, and S. Member, “Novel Pattern-Diversity-Based Decoupling Method and its Application to Multi-Element MIMO Antenna,” IEEE Trans. Antennas Propag., 2018. 22, (c), pp. 1–5.